Clinical Epigenetics

RESEARCH

Open Access

Mendelian randomization implicates causal association between epigenetic age acceleration and age-related eye diseases or glaucoma endophenotypes

Jiawei Chen[1,2], Xiang-Ling Yuan[1,3], Xiaoyu Zhou[2,4], Jiahao Xu[2,4], Xinyue Zhang[2,4] and Xuanchu Duan[1,2,4*]

Abstract

Background Age-related eye diseases (AREDs) have become increasingly prevalent with the aging population, serving as the leading causes of visual impairment worldwide. Epigenetic clocks are generated based on DNA methylation (DNAm) levels and are considered one of the most promising predictors of biological age. This study aimed to investigate the bidirectional causal association between epigenetic clocks and common AREDs or glaucoma endophenotypes.

Methods Instrumental variables for epigenetic clocks, AREDs, and glaucoma endophenotypes were obtained from corresponding genome-wide association study data of European descent. Bidirectional two-sample Mendelian randomization (MR) was employed to explore the causal relationship between epigenetic clocks and AREDs or glaucoma endophenotypes. Multivariable MR (MVMR) was used to determine whether glaucoma endophenotypes mediated the association of epigenetic clocks with glaucoma. Multiple sensitivity analyses were conducted to confirm the robustness of MR estimates.

Results The results showed that an increased intrinsic epigenetic age acceleration (HorvathAge) was significantly associated with an increased risk of primary open-angle glaucoma (OR = 1.04, 95% CI 1.02 to 1.06, $P = 6.1E{-}04$). The epigenetic age acceleration (EEA) of HannumAge was related to a decreased risk of primary angle-closure glaucoma (OR = 0.92, 95% CI 0.86 to 0.99, $P = 0.035$). Reverse MR analysis showed that age-related cataract was linked to decreased HannumAge ($\beta = -0.190$ year, 95% CI −0.374 to −0.008, $P = 0.041$). The EEA of HannumAge ($\beta = -0.85$ μm, 95% CI −1.57 to −0.14, $P = 0.019$) and HorvathAge ($\beta = -0.63$ μm, 95% CI −1.18 to −0.08, $P = 0.024$) were associated with decreased central corneal thickness (CCT). PhenoAge was related to an increased retinal nerve fiber layer thickness ($\beta = 0.06$ μm, 95% CI 0.01 to 0.11, $P = 0.027$). MVMR analysis found no mediation effect of CCT in the association of HannumAge and HorvathAge with glaucoma. DNAm-based granulocyte proportions were significantly associated with presbyopia, rhegmatogenous retinal detachment, and intraocular pressure ($P < 0.05$). DNAm-based plasminogen activator inhibitor-1 levels were significantly related to age-related macular degeneration and intraocular pressure ($P < 0.05$).

Conclusion The present study revealed a causal association between epigenetic clocks and AREDs. More research is warranted to clarify the potential mechanisms of the biological aging process in AREDs.

*Correspondence:
Xuanchu Duan
duanxchu@csu.edu.cn
Full list of author information is available at the end of the article

Keywords Glaucoma, Central corneal thickness, Age-related cataract, Biological aging, Epigenetic clock, Mendelian randomization

Introduction

Advanced aging is an important risk factor for a variety of common eye diseases that are collectively referred to as age-related eye diseases (AREDs), including glaucoma, age-related macular degeneration (AMD), age-related cataract (ARC), presbyopia, diabetic retinopathy (DR), rhegmatogenous retinal detachment (RRD), and retinal vascular occlusion (RVO) [1]. As the global population ages, AREDs are becoming increasingly prevalent, seriously threatening visual health around the world. It was projected that 587.6 million people would suffer from moderate and severe vision impairment (visual acuity < 6/18 but > 3/60 in the better eye), and 114.6 million people would be blind (visual acuity < 3/60) in 2050 globally [2]. Cataract and uncorrected refractive error were the two main global causes of avoidable blindness, whereas glaucoma, AMD, and DR were the leading global causes of irreversible blindness in people aged 50 years and older in 2020 [3]. Although natural aging seems necessary for AREDs development, many elderly people never develop the diseases in their entire lives, indicating the various ages at disease onset [4]. Individuals with the same chronological age can have inter-individual differences in the risk of AREDs due to different aging rates. Therefore, biological age may be a more effective predictor of disease risk associated with aging. Becker et al. thought that chronological age was an independent risk factor for AREDs, whereas biological age was the main driver of the diseases, which can be accelerated by environmental factors, lifestyle, and genetic variants [4].

Several common biomarkers were used to predict biological age, including epigenetic clocks, telomere length, transcriptomics, proteomics, metabolomics, and composite biomarker predictors [5]. Among them, the epigenetic clock, also known as DNA methylation age (DNAmAge), is regarded as one of the most promising predictors [6]. Epigenetic clocks measure the DNA methylation (DNAm) levels at specific cytosine-phosphate-guanine (CpG) loci, combined with regression analysis to evaluate biological age status. The first generation of epigenetic clocks comprises DNAm HorvathAge [7] and HannumAge [8], which are trained on chronological age. HorvathAge is the most widely used epigenetic clock tool, and it is also the first multi-tissue, all lifespans biological age estimator that utilizes 353 age-related CpGs assessed in 51 different tissues and cell types [6, 7]. Intrinsic epigenetic age acceleration (IEAA) is a derivative of the Horvath clock, which adjusts blood cell composition, and is considered a biomarker of cell-intrinsic aging [9]. HannumAge measures extrinsic aging based on 71 age-related CpGs from whole blood samples of adults [8, 9]. It can accurately predict biological age using blood samples collected from adults but has poor accuracy in non-blood tissues or from children [6]. The second generation of epigenetic clocks, including DNAm PhenoAge and GrimAge, are trained on a composite of biomarkers and, have an excellent ability to predict the morbidity and mortality risks of individuals [10, 11]. PhenoAge is based on 513 age-related CPGs from multiple clinical biomarkers and is strongly associated with mortality and behavioral lifestyle [10]. GrimAge was derived from 7 DNAm-based plasma protein markers associated with diseases, health, and smoking, resulting in better performance in predicting lifespan than other estimators [6, 11]. Epigenetic age acceleration (EAA) was used to describe the difference in DNAmAge from chronological age, reflecting the aging rate of individual organisms [12]. Although senescence is associated with AREDs, no research regarding the association between EAA or epigenetic clocks and AREDs has been conducted.

Mendelian randomization (MR) is an effective approach to investigate the potential causality between exposure factors and outcome phenotypes and has been widely applied to affirm the causal effect of diseases or risk factors on outcomes of interest. Based on the theory of random genetic variant allocation, MR analysis makes use of single nucleotide polymorphisms (SNPs) as instrumental variables (IVs) to derive causal estimations between two traits not affected by confounding effects and reverse causation [13]. Therefore, this study aimed to determine the causal association between epigenetic clocks and the risk of AREDs or glaucoma endophenotypes using bidirectional two-sample Mendelian randomization (TSMR) combined with multivariable Mendelian randomization (MVMR).

Methods

Study design

An outline of the study design and principles is shown in Fig. 1. Initially, we employed TSMR to evaluate the genetically predicted causality between epigenetic clocks and AREDs. In the forward TSMR analysis, epigenetic clocks were used as "exposure" variables and ocular diseases were used as "outcome" variables. Reverse TSMR analysis was performed using ocular diseases as "exposure"

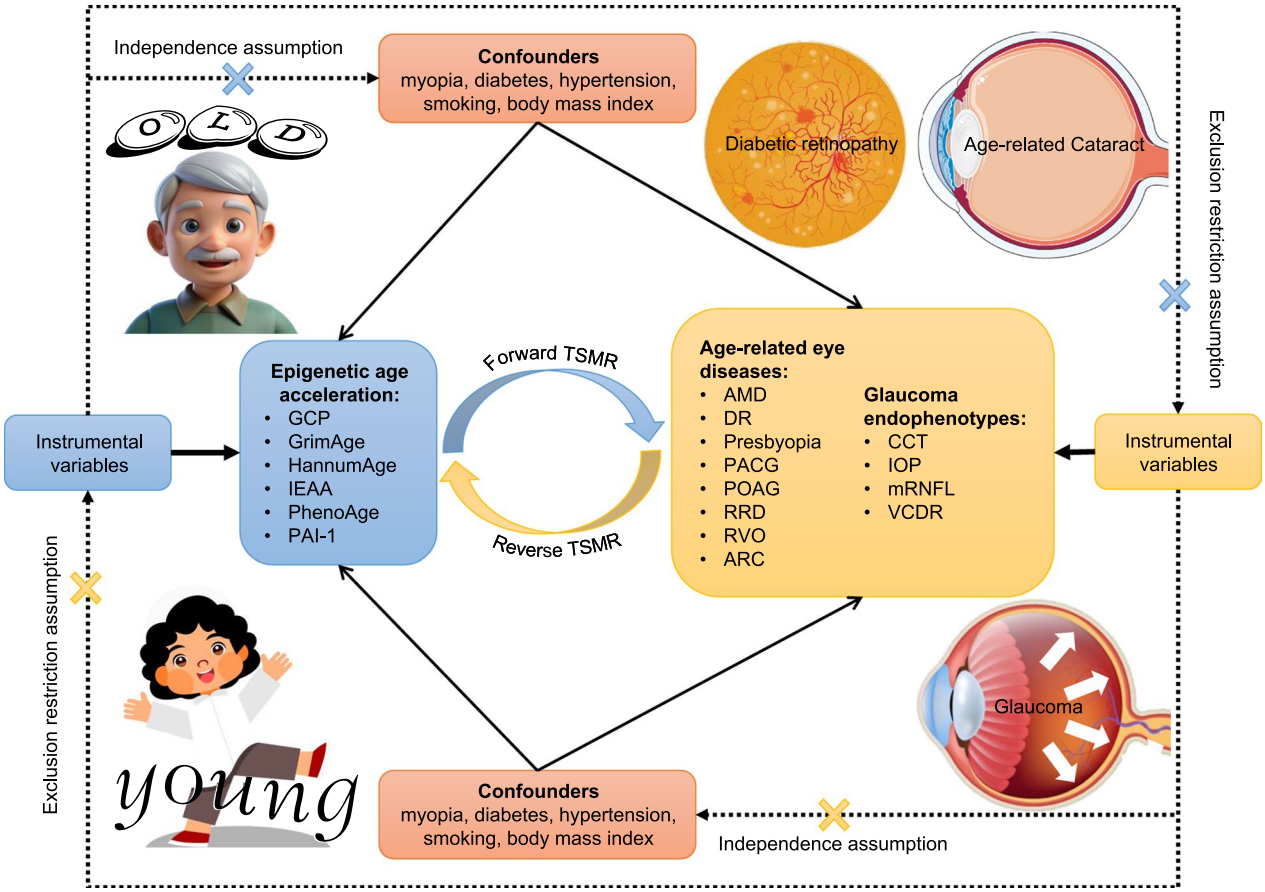

Fig. 1 The overview of the study design and principles of the present MR analysis. GCP, DNAm-based granulocyte proportions; IEAA, intrinsic epigenetic age acceleration; PAI-1, DNAm-based plasminogen activator inhibitor-1 levels; AMD, age-related macular degeneration; DR, diabetic retinopathy; PACG, primary angle-closure glaucoma; POAG, primary open-angle glaucoma; RRD, rhegmatogenous retinal detachment; RVO, retinal vascular occlusion; ARC, age-related cataract; CCT, central corneal thickness; IOP, intraocular pressure; mRNFL, macular retinal nerve fiber layer thickness; VCDR, vertical cup-to-disk ratio

variables and epigenetic clocks as "outcome" variables. Then, we further explored the causal association between epigenetic clocks and glaucoma endophenotypes since a significant relationship was identified between epigenetic aging and glaucoma. MVMR was applied to investigate the mediation effect of glaucoma endophenotypes on the association of epigenetic clocks with glaucoma. MR analysis relies on three key assumptions as follows [14]: (1) Relevance assumption: IVs must be strongly associated with exposure phenotype. (2) Independence assumption: IVs should be independent of potential confounders. (3) Exclusion restriction assumption: IVs solely affect outcomes through predicted exposure.

Data sources

Table 1 summarizes the data sources for all phenotypes in the MR analysis. The genome-wide association studies (GWAS) data for four epigenetic clocks, including PhenoAge, GrimAge, HannumAge, and IEAA (HorvathAge), were obtained from a recent meta-analysis comprising a total of 34,710 European ancestry participants from 28 cohorts [15]. This GWAS meta-analysis successfully identified 137 genetic variants representing DNA methylation biomarkers of biological aging. We also included two important DNA methylation-based biomarkers, namely DNA methylation proxies for granulocyte proportions (GCP) and plasminogen activator inhibitor-1 (PAI-1) levels [15]. Neutrophils, the main components of granulocytes, are considered pathogenic mediators and biomarkers of AREDs [16]. Previous studies have shown that PAI-1 might contribute to the pathogenesis of glaucoma, AMD, and DR [17, 18].

Eight common AREDs, including AMD, ARC, presbyopia, primary angle-closure glaucoma (PACG), primary open-angle glaucoma (POAG), RRD, RVO, and DR, were considered in this MR study. The genetic instruments for these eight ocular diseases (AMD: 9721 cases, and 381,339 controls; ARC: 65,235 cases, and 341,546

Table 1 Data sources for MR analyses in this study

Phenotypes	Cases	Controls	Sample size	Ancestry	Source	Pubmed ID
Epigenetic age acceleration	–	–	34,710	European	Edinburgh DataShare	34187551
Age-related macular degeneration	9721	381,339	391,060	European	FinnGen study R10	36653562
Age-related cataract	65,235	341,546	406,781			
Presbyopia	1597	394,028	395,625			
Primary angle-closure glaucoma	1307	391,275	392,582			
Primary open-angle glaucoma	8530	391,275	399,805			
Rhegmatogenous retinal detachment	4024	376,650	380,674			
Retinal vascular occlusion	3635	376,650	380,285			
Diabetic retinopathy	10,413	308,633	319,046	European	FinnGen study R9	36653562
Central corneal thickness	–	–	16,204	European	International Glaucoma Genetic Consortium	31798171
Intraocular pressure	–	–	31,269			
Vertical cup-to-disk ratio	–	–	25,180			
Macular retinal nerve fiber layer thickness	–	–	31,434	European	UK biobank	33979322

controls; presbyopia: 1597 cases, and 394,028 controls; PACG: 1,307 cases, and 391,275 controls; POAG: 8530 cases, and 391,275 controls; RRD: 4024 cases, and 376,650 controls; RVO: 3635 cases, and 376,650 controls; DR, 10,413 cases, and 308,633 controls) were acquired from the FinnGen study based on European-descent individuals [19]. The FinnGen study is a large-scale genomics initiative that has analyzed over 500,000 Finnish biobank samples and correlated genetic variations with health data to elucidate disease mechanisms and predispositions [19].

Central corneal thickness (CCT), intraocular pressure (IOP), vertical cup-to-disk ratio (VCDR), and macular retinal nerve fiber layer (mRNFL) thickness are the four main endophenotypes of glaucoma. The summary data for CCT (16,204 individuals), IOP (31,269 individuals), and VCDR (25,180 individuals) were collected from a multi-trait GWAS study involving European ancestry participants via the GWAS Catalog (https://www.ebi.ac.uk/gwas/) [20]. The genetic instruments for mRNFL were extracted from a GWAS study of inner retinal morphology based on optical coherence tomography (OCT) images of 31,434 European ancestry participants from the UK Biobank [21].

Selection of instrumental variables

To meet the relevance assumption, SNPs associated with each exposure at genome-wide significance ($P < 5 \times 10^{-8}$) level were extracted as IVs. Due to the lack of effective IVs, the threshold of the P value was loosened to 5×10^{-6} for the four epigenetic clocks, and 1×10^{-6} for GCP and PAI-1, similar to prior studies [22, 23]. For the same reason, the P value threshold for IVs selection was set at 5×10^{-7} for DR, CCT, and IOP, 5×10^{-6} for AMD, presbyopia, and RD, as well as 5×10^{-5} for PACG and RVO. We preserved the SNPs without linkage disequilibrium (LD) using criteria of $r^2 < 0.001$ and clumping distance > 10 Mb based on the European 1000 Genomes for subsequent analysis. To filter high-quality IVs, we excluded SNPs with potentially low confidence (MAF < 0.01), weak instrumental variables (F-statistics < 10), ambiguous and palindromic SNPs, or SNPs potentially associated with outcome ($P < 0.01$) [24]. For each single variant, the F-statistics was calculated using the formula $F = \frac{\beta^2}{SE^2}$, and the proportion of variance in the exposure explained by the genetic variants (R^2) was calculated using the formula $R^2 = 2 \times MAF \times (1 - MAF) \times \beta^2$, where β is the genetic association with exposure (SE, standard error for β; MAF, minor allele frequency) [25, 26]. In addition, Steiger filtering was performed to ensure the correct direction from exposure to the outcome [27]. We searched the Ensembl database (https://www.ensembl.org/) and deleted the SNPs associated with underlying confounding risk factors (including myopia, diabetes, hypertension, smoking, and body mass index) affecting epigenetic clocks and AREDs. Proxy SNPs were not used to avoid bringing in unpredicted bias in this study [28].

Mendelian randomization analysis

For the TSMR analysis, we used the inverse-variance weighted (IVW) with a multiplicative random-effects model as the primary approach to determine the causal associations between epigenetic clocks and AREDs or glaucoma endophenotypes. The MR-pleiotropy residual sum and outlier (MR-PRESSO), MR-Egger, and Weighted median served as supplementary methods to evaluate the robustness of the MR estimations. The direct effect (β_a) of epigenetic clocks on CCT was derived from TSMR. MVMR-IVW was performed to assess the direct effect

(β_b) of CCT on glaucoma. The mediation effect was calculated using the formula of $\beta_{med} = \beta_a \times \beta_b$, where $SE_{med} = \sqrt{\beta_a^2 \times SE_b^2 + \beta_b^2 \times SE_a^2}$, $Z_{med} = \frac{\beta_{med}}{SE_{med}}$, and P_{med} were derived from the Z score table [29].

Cochran's Q test was conducted to assess heterogeneity among SNPs using the IVW and MR-Egger methods [30]. The random-effects model of the IVW method can address the effect of heterogeneity and accurately make causal estimations [31]. Horizontal pleiotropy of IVs was detected using MR-Egger intercept and MR-PRESSO Global test. Significant horizontal pleiotropy indicates the existence of an alternative pathway that allows IVs of exposure to affect the outcome, which violates the exclusion restriction assumption of MR analysis. Additionally, scatter plots, funnel plots, and leave-one-out analyses were used to visualize potential heterogeneity and pleiotropy. The statistical power was calculated using an online calculator (https://sb452.shinyapps.io/power/) [32].

Statistical analysis

A two-sided significance threshold of $P < 0.05$ was applied to all statistical analyses. All MR analyses were conducted using the "TwoSampleMR" package (Version 0.6.3) [33], "MendelianRandomization" package (Version 0.9.0) [34], or "MVMR" package (Version 0.4) [35] in R software (Version 4.3.2; https:// www.R-project.org/).

Results

Instrumental variables selection

After the rigorous filtering procedure, we screened 41, 56, 35, 27, 32, and 36 qualified SNPs as IVs for HannumAge (F-statistics range 21 to 99), IEAA (F-statistics range 21 to 240), PhenoAge (F-statistics range 21 to 89), GrimAge (F-statistics range 21 to 45), GCP (F-statistics range 18 to 76), and PAI-1 (F-statistics range 20 to 163), respectively. For ocular diseases, 64, 32, 23, 85, 46, 16, 84, and 40 qualified SNPs were selected as IVs for AMD (F-statistics range 21 to 1008), DR (F-statistics range 26 to 1283), presbyopia (F-statistics range 21 to 26), PACG (F-statistics range 17 to 28), POAG (F-statistics range 30 to 200), RRD (F-statistics range 21 to 40), RVO (F-statistics range 16 to 32), and ARC (F-statistics range 30 to 257), respectively. For glaucoma endophenotypes, 37, 20, 28, and 22 qualified SNPs were chosen as IVs for CCT (F-statistics range 26 to 257), IOP (F-statistics range 25 to 75), mRNFL (F-statistics range 30 to 115), and VCDR (F-statistics range 29 to 207), respectively. The F-statistics of all IVs were > 10, indicating that the MR estimations were not biased by weak instrumental variables.

Causal association between epigenetic aging and age-related eye diseases

Forward TSMR analysis showed that genetically predicted HannumAge was significantly associated with PACG (IVW: odds ratio [OR] = 0.92, 95% confidence interval [CI] 0.86 to 0.99, $P = 0.035$; Table 2). An increase in genetically predicted IEAA was significantly associated with an increased risk of POAG (IVW: OR = 1.04, 95% CI 1.02 to 1.06, $P = 6.1E\text{-}04$). Increased DNAm-based PAI-1 levels was significantly associated with an increased risk of AMD (IVW: OR = 1.00006, 95% CI 1.000002 to 1.0001, $P = 0.042$). The DNAm-based estimate of GCP was significantly associated with presbyopia (IVW: OR = 0.010, 95% CI 0.0002 to 0.522, $P = 0.022$) and RRD (IVW: OR = 26.64, 95% CI 2.70 to 263.05, $P = 0.005$). The reverse TSMR analysis revealed that genetic predisposition to ARC was significantly associated with an increase in HannumAge (IVW: $\beta = -0.190$, 95% CI −0.374 to −0.008, $P = 0.041$). We did not find any significant associations between epigenetic clocks and other AREDs (Fig. 2, Tables S1 and S4).

We had high statistical powers (power > 80%) for the causal estimations from IEAA on POAG, GCP on RRD, and ARC on HannumAge, but moderate statistical powers were shown for the causal estimations from HannumAge on PACG, PAI-1 on AMD, and GCP on presbyopia (Table 2). Although the MR-Egger intercept indicated potential pleiotropy in the causality from HannumAge on PACG, this could not be confirmed by the MR-PRESSO Global test. No significant heterogeneity or pleiotropy affected the other significant associations between epigenetic clocks and ocular diseases.

Causal association between epigenetic aging and *glaucoma* endophenotypes

In the forward TSMR analysis, genetic liability for increased HannumAge (IVW: $\beta = -0.85$ μm, 95% CI −1.57 to −0.14, $P = 0.019$) and IEAA (IVW: $\beta = -0.63$μm, 95% CI -1.18 to -0.08, $P = 0.024$) was significantly associated with decreased CCT (Table 3). Genetically predicted PhenoAge was significantly associated with mRNFL (IVW: $\beta = 0.06$ μm, 95% CI 0.01 to 0.11, $P = 0.027$). Genetic liability for the DNAm-based estimate of GCP (IVW: $\beta = -3.03$ mmHg, 95% CI −5.86 to −0.20, $P = 0.036$) and PAI-1 (IVW: $\beta = 0.0001$mmHg, 95% CI 0.00002 to 0.0002, $P = 0.015$) was significantly associated with IOP. Reverse TSMR analysis showed that genetically predicted IOP was significantly associated with PAI-1 (IVW: $\beta = 0.26$, 95% CI 0.01 to 0.50, $P = 0.041$). No significant associations between epigenetic clocks and other glaucoma endophenotypes were observed (Fig. 3, Tables S7 and S10). All statistical powers of the

Table 2 Significant causal associations between epigenetic age acceleration and age-related eye diseases estimated using bidirectional TSMR

Exposure	Outcome	SNPs	Method	OR (95% CI)	*P*	P_Q	P_{Int}	P_G	Power (%)
HannumAge	PACG	41	IVW	0.92 (0.86 to 0.99)	0.035	0.510	0.020	0.502	65.0
			MR-Egger	0.75 (0.62 to 0.90)	0.004				
			MR-PRESSO	0.92 (0.86 to 0.99)	0.039				
			WM	0.90 (0.81 to 1.01)	0.068				
IEAA	POAG	54	IVW	1.04 (1.02 to 1.06)	6.1E-04	0.732	0.300	0.743	96.5
			MR-Egger	1.02 (0.97 to 1.06)	0.521				
			MR-PRESSO	1.04 (1.02 to 1.06)	5.7E-04				
			WM	1.03 (0.996 to 1.060)	0.084				
PAI-1	AMD	33	IVW	1.00006 (1.000002 to 1.0001)	0.042	0.291	0.510	0.335	69.3
			MR-Egger	1.00007 (1.000005 to 1.0001)	0.042				
			MR-PRESSO	1.00006 (1.000002 to 1.0001)	0.050				
			WM	1.00004 (0.999959 to 1.0001)	0.320				
GCP	Presbyopia	27	IVW	0.010 (0.0002 to 0.522)	0.022	0.313	0.211	0.341	70.6
			MR-Egger	0.00003 (1.69E-09 to 0.494)	0.046				
			MR-PRESSO	0.010 (0.0002 to 0.522)	0.031				
			WM	0.003 (0.00001 to 0.603)	0.032				
GCP	RRD	29	IVW	26.64 (2.70 to 263.05)	0.005	0.564	0.617	0.613	82.9
			MR-Egger	6.70 (0.02 to 2256.62)	0.527				
			MR-PRESSO	26.64 (2.91 to 243.72)	0.007				
			WM	22.27 (0.83 to 598.38)	0.065				
ARC	HannumAge	31	IVW	0.83 (0.69 to 0.99)	0.041	0.988	0.708	0.988	100
			MR-Egger	0.75 (0.45 to 1.26)	0.289				
			MR-PRESSO	0.83 (0.72 to 0.94)	0.008				
			WM	0.86 (0.66 to 1.12)	0.259				

AMD, age-related macular degeneration; PACG, primary angle-closure glaucoma; POAG, primary open-angle glaucoma; RRD, rhegmatogenous retinal detachment; ARC, age-related cataract; PAI-1, DNAm-based plasminogen activator inhibitor-1 levels; GCP, DNAm-based granulocyte proportions; IEAA, intrinsic epigenetic age acceleration; TSMR, two-sample Mendelian randomization; IVW, inverse-variance weighted; MR-PRESSO, Mendelian randomization pleiotropy residual sum and outlier; WM, weighted median; OR, odds ratio; 95% CI, 95% confidence interval; P_Q was the *P* value derived from Cochran's Q test using IVW method. P_{Int} was the *P* value derived from MR-Egger intercept. P_G was the *P* value derived from MR-PRESSO global test. $P < 0.05$ was considered as statistically significant

significant causal estimations between epigenetic clocks and glaucoma endophenotypes were 100%. We found no heterogeneity or pleiotropy in the significant associations between epigenetic clocks and glaucoma endophenotypes (Table 3).

Mediation effect of *glaucoma* endophenotypes

MVMR analysis showed that the association of HannumAge with PACG lost statistical significance after adjusting for CCT (Table 4). Genetically predicted IEAA was still significantly associated with POAG after adjusting for CCT (IVW: OR = 0.967, 95% CI 0.939 to 0.997, $P = 0.029$). Heterogeneity was observed in the MVMR analysis of IEAA, CCT, and POAG. No significant pleiotropy was observed in all MVMR analyses. However, we found no significant mediation effect of CCT on the association between epigenetic clocks and glaucoma (Table 5).

Discussion

As one of the common and important AREDs, glaucoma is a group of optic neurodegenerative diseases associated with pathologically increased IOP [36]. Primary glaucoma can be classified as POAG and PACG according to the status of the anterior chamber angle when IOP is raised. It was projected that approximately 112 million people would suffer from glaucoma worldwide in 2040, including nearly 80 million POAG patients and 32 million PACG patients [37]. Advanced age is the second most critical risk factor for glaucoma in addition to IOP elevation. A meta-analysis showed that, with each decade increase in age beyond 40 years, the OR for POAG was 1.73 (95% CI 1.63–1.82) after adjusting for gender, habitation type, response rate, and year of study conducted [37], and the OR for PACG was 2.18 (95% CI 1.89–2.54) in Asia [38]. In the present study, we systemically investigated the bidirectional causal associations between

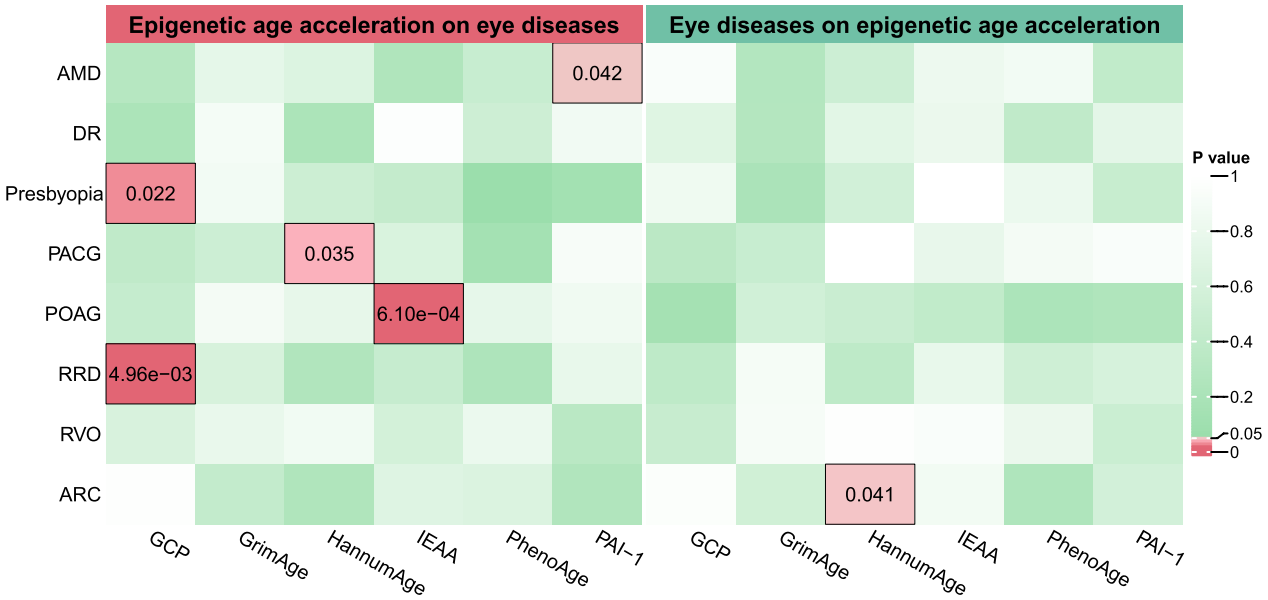

Fig. 2 MR estimated the causal association between epigenetic age acceleration and age-related eye diseases using the inverse-variance weighted method. GCP, DNAm-based granulocyte proportions; IEAA, intrinsic epigenetic age acceleration; PAI-1, DNAm-based plasminogen activator inhibitor-1 levels; AMD, age-related macular degeneration; DR, diabetic retinopathy; PACG, primary angle-closure glaucoma; POAG, primary open-angle glaucoma; RRD, rhegmatogenous retinal detachment; RVO, retinal vascular occlusion; ARC, age-related cataract; $P < 0.05$ was considered statistically significant

genetically predicted epigenetic clocks and the eight most common AREDs, as well as four glaucoma endophenotypes. Our findings showed that genetically predicted IEAA was significantly associated with a higher risk of POAG, and genetically predicted EEA of HannumAge was significantly related to a lower risk of PACG. Genetically predicted EEA of HannumAge and IEAA were also significantly associated with decreased CCT. MR analysis showed significant bidirectional causality between genetically predicted PAI-1 and IOP. Based on a comprehensive literature search of Pubmed and Web of Science, this study is the first MR analysis coupled with large-scale GWAS data to comprehensively determine the causal relationship between epigenetic clocks and AREDs. The findings of our study suggested the contribution of genetically predicted DNAmAge on the risk of AREDs and the age-related changes of glaucomatous endophenotypes.

Our study revealed that the OR for POAG was 1.04 (95% CI 1.02–1.06) with each year increase in genetically predicted IEAA, which was equal to 1.48 (95% CI 1.22–1.79) with each decade increase in genetically predicted IEAA, highlighting the effect of cell-intrinsic aging on glaucoma. The accumulation of senescent cells is a basic physiological and pathological change during body aging. Many studies have indicated the critical contribution of cellular senescence to the development of glaucoma since increased levels of senescence biomarkers, such as senescence-associated beta-galactosidase (SA-β-gal), senescence-associated secretory phenotype [SASP, including interleukin-6 (IL-6), IL-1β, IL-8, transforming growth factor beta1 (TGF-β1) and vascular endothelial growth factor-α (VEGF-α)], and ungraded expression of senescence-associated genes (including $p16^{INK4a}$, $p21^{WAF-1}$, p53, and $p15^{INK4b}$) were found in TM cells and retinal ganglion cells (RGCs) in patients with glaucoma [39]. Elevated IOP is in connection with the upregulation of $p16^{INK4a}$ and increased expression of SASP [40, 41]. In addition, age retinas are susceptible to high-IOP induced damages, such as loss of RGCs and functional changes [4, 42]. Elimination of senescent cells and knockout of senescence-associated genes have been proposed as effective therapeutic approaches for preventing RGCs death, alleviating structural damages, and improving visual function [40, 43, 44].

As an important biomarker of aging, DNA methylation has been suggested to be associated with glaucoma development by growing evidence. A higher level of DNA methylation was found in glaucomatous lamina cribrosa cells and TM cells [45, 46]. A DNA methylation study by Cai et al. revealed differential DNA methylation patterns in human Schlemm's canal endothelial cells with glaucoma and identified differentially methylated regions of glaucoma-related genes, including TBX3, TNXB1, DAXX, and PITX2 [47]. Wan et al. delineated the crucial effect of hypomethylation on growth differentiation factor 7 (GDF7) in aqueous humor outflow obstruction

Table 3 Significant causal associations between epigenetic age acceleration and glaucoma endophenotypes estimated using bidirectional TSMR

Exposure	Outcome	SNPs	Method	Beta (95% CI)	*P*	P_Q	P_{Int}	P_G	Power (%)
HannumAge	CCT	41	IVW	−0.85 (−1.57 to −0.14)	0.019	0.900	0.343	0.906	100
			MR-Egger	−1.65 (−3.43 to 0.13)	0.077				
			MR-PRESSO	−0.85 (−1.46 to −0.24)	0.009				
			WM	−0.86 (−1.89 to 0.17)	0.101				
IEAA	CCT	55	IVW	−0.63 (−1.18 to −0.08)	0.024	0.694	0.781	0.693	100
			MR-Egger	−0.46 (−1.74 to 0.82)	0.480				
			MR-PRESSO	−0.63 (−1.15 to −0.11)	0.021				
			WM	−0.49 (−1.28 to 0.29)	0.218				
PhenoAge	mRNFL	34	IVW	0.06 (0.01 to 0.11)	0.027	0.692	0.153	0.698	100
			MR-Egger	−0.02 (−0.13 to 0.10)	0.770				
			MR-PRESSO	0.06 (0.01 to 0.11)	0.023				
			WM	0.05 (−0.03 to 0.13)	0.200				
GCP	IOP	30	IVW	−3.03 (−5.86 to −0.20)	0.036	0.210	0.417	0.200	100
			MR-Egger	−5.93 (−13.40 to 1.53)	0.130				
			MR-PRESSO	−3.03 (−5.86 to −0.20)	0.044				
			WM	−2.97 (−6.99 to 1.05)	0.147				
PAI-1	IOP	36	IVW	0.0001 (0.00002 to 0.0002)	0.015	0.496	0.753	0.523	100
			MR-Egger	0.0001 (0.00001 to 0.0002)	0.042				
			MR-PRESSO	0.0001 (0.00002 to 0.0002)	0.019				
			WM	0.0001 (−0.00005 to 0.0002)	0.259				
IOP	PAI-1	18	IVW	0.26 (0.01 to 0.50)	0.041	0.326	0.767	0.317	100
			MR-Egger	0.40 (−0.56 to 1.36)	0.429				
			MR-PRESSO	0.26 (0.01 to 0.50)	0.057				
			WM	0.20 (−0.14 to 0.53)	0.257				

CCT, central corneal thickness; IOP, intraocular pressure; mRNFL, macular retinal nerve fiber layer thickness; PAI-1, DNAm-based plasminogen activator inhibitor-1 levels; GCP, DNAm-based granulocyte proportions; IEAA, intrinsic epigenetic age acceleration; TSMR, two-sample Mendelian randomization; IVW, inverse-variance weighted; MR-PRESSO, Mendelian randomization pleiotropy residual sum and outlier; WM, weighted median; OR, odds ratio; 95% CI, 95% confidence interval; P_Q was the *P* value derived from Cochran's Q test using IVW method. P_{Int} was the *P* value derived from MR-Egger intercept. P_G was the *P* value derived from MR-PRESSO global test. $P < 0.05$ was considered as statistically significant

and confirmed that GDF7 neutralization therapy could effectively control IOP [48]. Reprograming age-associated epigenetic modifications has been shown to reverse vision loss in glaucoma mouse models and in aged mice [49]. In the present study, DNA methylation IEAA was significantly associated with an increased risk of POAG, suggesting that the epigenetic clock could be a potential predictor of glaucoma risk and detect retinal or optic damage in patients with glaucoma. Unexpectedly, the genetically predicted EEA of HannumAge was related to a decreased risk of PACG. HannumAge is a single-tissue (whole blood sample) DNAmAge estimator that reflects age-dependent changes in cell type composition [9]. Observational studies have suggested that changes in the composition of blood cells are involved in the pathogenesis and development of PACG. A higher red blood cell distribution width (RDW) was found in PACG patients, and an increased RDW was associated with the severity of PACG [50]. The neutrophil-to-lymphocyte ratio was significantly greater in the peripheral blood of patients with PACG than in the controls [51]. However, the causal association between the EEA of HannumAge and PACG should be interpreted with caution because potential pleiotropy was observed by the MR-Egger intercept but not the MR-PRESSO global test.

Evaluating the relationship between epigenetic clocks and glaucoma endophenotypes would help clarify the impact of epigenetic clocks on glaucoma. A thin cornea is considered an underlying risk factor for glaucoma [52]. Our analysis showed that the genetically predicted EEA of HannumAge and IEAA were significantly related to decreased CCT, possibly indicating an increased risk of glaucoma mediated by CCT. However, we did not observe any significant mediation effect of CCT on the causality from HannumAge on PACG, and IEAA on POAG. More studies are required to clarify the meaning of decreased CCT with aging in patients with glaucoma. RNFL thinning and enlarged VCDR

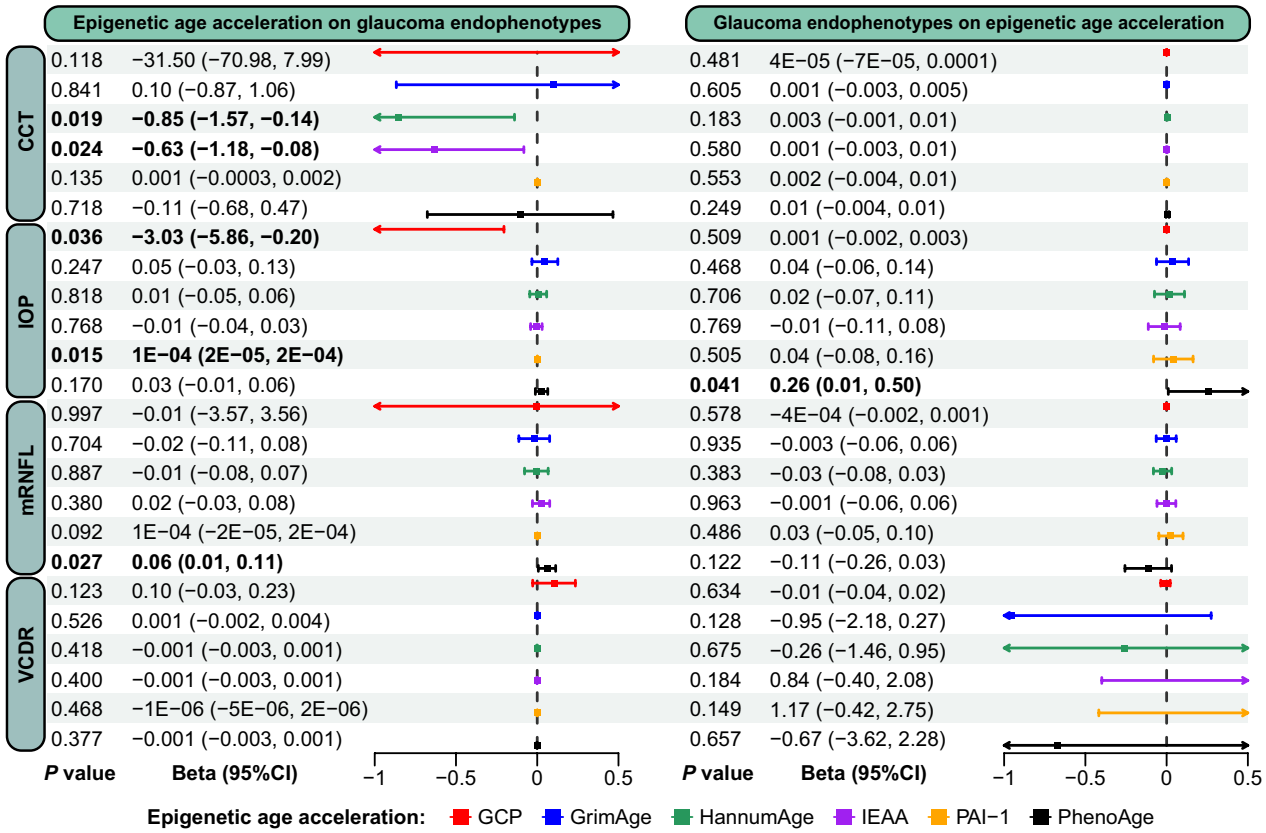

Fig. 3 MR estimated the causal association between epigenetic age acceleration and glaucoma endophenotypes using the inverse-variance weighted method. GCP, DNAm-based granulocyte proportions; IEAA, intrinsic epigenetic age acceleration; PAI-1, DNAm-based plasminogen activator inhibitor-1 levels; CCT, central corneal thickness; IOP, intraocular pressure; mRNFL, macular retinal nerve fiber layer thickness; VCDR, vertical cup-to-disk ratio; 95% CI, 95% confidence interval; $P < 0.05$ was considered statistically significant

Table 4 Casual association between epigenetic age acceleration and glaucoma adjusting CCT using multivariable MR

Exposure	Outcome	SNPs	Method	OR (95% CI)	*P*	F-statistic	Heterogeneity	Pleiotropy
HannumAge	PACG	79	IVW	0.997 (0.916 to 1.085)	0.941	15	Q = 98, *P* = 0.051	Intercept = −0.0096, se = 0.0085, *P* = 0.259
			MR-Egger	1.041 (0.93 to 1.166)	0.485			
			LASSO	0.991 (0.915 to 1.074)	0.827			
CCT			IVW	1.001 (0.996 to 1.006)	0.762	23		
			MR-Egger	1.001 (0.995 to 1.006)	0.843			
			LASSO	1.002 (0.997 to 1.007)	0.511			
IEEA	POAG	89	IVW	0.967 (0.939 to 0.997)	0.029	23	Q = 178, *P* = 3.0E−08	Intercept = −0.0003, se = 0.0044, *P* = 0.947
			MR-Egger	0.968 (0.927 to 1.011)	0.147			
			LASSO	0.974 (0.954 to 0.995)	0.017			
CCT			IVW	1.002 (0.999 to 1.005)	0.130	19		
			MR-Egger	1.002 (0.999 to 1.005)	0.132			
			LASSO	1.006 (1.004 to 1.009)	1.9E−06			

PACG, primary angle-closure glaucoma; POAG, primary open-angle glaucoma; CCT, central corneal thickness; IEAA, intrinsic epigenetic age acceleration; IVW, inverse-variance weighted; MR, Mendelian randomization. $P < 0.05$ was considered as statistically significant

are the direct signs of RGCs loss caused by IOP elevation [36]. An unexpected association was observed between the genetically predicted EEA of PhenoAge and increased mRNFL thickness in this study. Yet, it should be interpreted prudently due to the contrary effect direction estimated by MR-Egger. Retrospective

Table 5 Mediation effect of central corneal thickness in the association between epigenetic age acceleration and glaucoma

Exposure	Mediator	Outcome	Total effect[a]			Direct effect[b]			Mediation effect			
			Beta	SE	P_{IVW}	Beta	SE	P_{IVW}	Effect	SE	P_{med}	Proportion (%)
HannumAge	CCT	PACG	−0.080	0.038	0.035	−0.003	0.043	0.941	−0.0007	0.0023	0.382	0.88
IEAA	CCT	POAG	0.037	0.011	6.10E−04	−0.033	0.015	0.029	−0.0014	0.0011	0.104	3.78

PACG, primary angle-closure glaucoma; POAG, primary open-angle glaucoma; CCT, central corneal thickness; IEAA, intrinsic epigenetic age acceleration; IVW, inverse-variance weighted; P_{med} was derived from Z score table. $P < 0.05$ was considered as statistically significant

a. The causal effects of epigenetic aging on glaucoma derived from univariable two-sample MR analyses

b. The causal effects of epigenetic aging on glaucoma derived from multivariable MR analyses

studies have shown a significant decline in RNFL thickness with aging (range −0.20 μm to −0.70 μm per year) [53–55]. This unexpectedly inconsistent finding between MR analysis and observational research should be addressed in future studies. A bidirectional causal association between increased DNAm-based PAI-1 levels and increased IOP was revealed by this MR analysis. Higher levels of DNAm-based PAI-1 were found to be associated with hypertension, diabetes, coronary heart disease, and early age at menopause, whereas lower levels were related to disease-free status and better physical functioning [11]. These findings suggest that high PAI-1 level could be a potential explanation for the association between systemic diseases and elevated IOP or glaucoma risk.

PAI-1 is the main substance that inhibits fibrinolytic activity in blood circulation, and an increase in PAI-1 levels can lead to a decrease in fibrinolytic activity, thus increasing the risk of thrombosis. However, we did not observe a significant association between genetically predicted PAI-1 and RVO. The annual incidence of AMD is 0.03% in people aged 55 to 59 years, increasing to 3.67% in people aged 90 years or older [56]. DNA methylation estimated PAI-1 level was related to an increased risk of AMD, but the OR was relatively small. This was consistent with the findings of previous studies showing that PAI-1 could induce the development of choroidal experimental neovascularization in AMD, suggesting a potential therapeutic approach of targeting PAI-1 in neovascular AMD [18]. DNA methylation estimated GCP was associated with a decreased risk of presbyopia in this study. Presbyopia is the result of the declined accommodation of the ciliary muscle and lens [57]. Our findings raise concerns about the effect of age-associated inflammation on the development of presbyopia. However, genetically predicted GCP was also associated with an increased risk of RRD, with a meaningful OR value, suggesting that age-associated inflammation greatly contributed to the development of RRD. Maidana et al. found that peripheral monocytes and neutrophils were responsible for photoreceptor degeneration in an experimental retinal detachment model, highlighting the important role of immune cell infiltration in the pathogenesis of retinal detachment [58].

There are inevitable limitations to our study. First, this study was based on summary GWAS data derived from European ancestry population, raising concerns over the generalizability of the findings to other ethnic populations. Second, although all four epigenetic clocks represent DNA methylation-based biological age, they did not show consistent results in the relationship with AREDs because they were trained using different approaches. There is currently a lack of an epigenetic clock that can accurately assess the biological age of ocular tissues. Finally, genetic variants can only explain a portion of the variability in epigenetic clocks and AREDs; thus, environmental factors and lifestyle should be considered when evaluating the complex interaction between DNAmAge and AREDs.

Conclusion

The present study demonstrated a causal association between accelerated epigenetic clocks, age-associated PAI-1 levels, GCP, and the risk of AREDs, as well as changes in glaucoma endophenotypes. More studies are required to elucidate the mechanisms underlying the biological aging effect on AREDs.

Supplementary Information

The online version contains supplementary material available at https://doi.org/10.1186/s13148-024-01723-w.

Additional file 1: Fig. S1. Scatter plots of significant MR estimations between epigenetic age acceleration and age-related eye diseases. (**a**) HannumAge on primary angle-closure glaucoma; (**b**) intrinsic epigenetic age acceleration on primary open-angle glaucoma; (**c**) DNAm-based plasminogen activator inhibitor-1 levels on age-related macular degeneration; (**d**) DNAm-based granulocyte proportions on presbyopia; (**e**) DNAm-based granulocyte proportions on rhegmatogenous retinal detachment; (**f**) age-related cataract on HannumAge. **Fig. S2.** Funnel plots of significant MR estimations between epigenetic age acceleration and age-related eye diseases. (**a**) HannumAge on primary angle-closure glaucoma; (**b**) intrinsic epigenetic age acceleration on primary open-angle glaucoma; (**c**) DNAm-based plasminogen activator inhibitor-1 levels on age-related macular degeneration; (**d**) DNAm-based granulocyte proportions on presbyopia;

(**e**) DNAm-based granulocyte proportions on rhegmatogenous retinal detachment; (**f**) age-related cataract on HannumAge. **Fig. S3.** Leave-one-out plots of significant MR estimations between epigenetic age acceleration and age-related eye diseases. (**a**) HannumAge on primary angle-closure glaucoma; (**b**) intrinsic epigenetic age acceleration on primary open-angle glaucoma; (**c**) DNAm-based plasminogen activator inhibitor-1 levels on age-related macular degeneration; (**d**) DNAm-based granulocyte proportions on presbyopia; (**e**) DNAm-based granulocyte proportions on rhegmatogenous retinal detachment; (**f**) age-related cataract on HannumAge. **Fig. S4.** Scatter plots of significant MR estimations between epigenetic age acceleration and glaucoma endophenotypes. (**a**) HannumAge on central corneal thickness; (**b**) intrinsic epigenetic age acceleration on central corneal thickness; (**c**) PhenoAge on macular retinal nerve fiber layer thickness; (**d**) DNAm-based granulocyte proportions on intraocular pressure; (**e**) DNAm-based plasminogen activator inhibitor-1 levels on intraocular pressure; (**f**) intraocular pressure on DNAm-based plasminogen activator inhibitor-1 levels. **Fig. S5.** Funnel plots of significant MR estimations between epigenetic age acceleration and glaucoma endophenotypes. (**a**) HannumAge on central corneal thickness; (**b**) intrinsic epigenetic age acceleration on central corneal thickness; (**c**) PhenoAge on macular retinal nerve fiber layer thickness; (**d**) DNAm-based granulocyte proportions on intraocular pressure; (**e**) DNAm-based plasminogen activator inhibitor-1 levels on intraocular pressure; (**f**) intraocular pressure on DNAm-based plasminogen activator inhibitor-1 levels. **Fig. S6.** Leave-one-out plots of significant MR estimations between epigenetic age acceleration and glaucoma endophenotypes. (**a**) HannumAge on central corneal thickness; (**b**) intrinsic epigenetic age acceleration on central corneal thickness; (**c**) PhenoAge on macular retinal nerve fiber layer thickness; (**d**) DNAm-based granulocyte proportions on intraocular pressure; (**e**) DNAm-based plasminogen activator inhibitor-1 levels on intraocular pressure; (**f**) intraocular pressure on DNAm-based plasminogen activator inhibitor-1 levels.

Additional file 2: Table S1. Mendelian randomization estimations between epigenetic aging and age-related eye diseases. **Table S2.** Heterogeneity of Mendelian randomization estimations between epigenetic aging and age-related eye diseases. **Table S3.** Pleiotropy of Mendelian randomization estimations between epigenetic aging and age-related eye diseases. **Table S4.** Mendelian randomization estimations between age-related eye diseases and epigenetic aging. **Table S5.** Heterogeneity of Mendelian randomization estimations between age-related eye diseases and epigenetic aging. **Table S6.** Pleiotropy of Mendelian randomization estimations between age-related eye diseases and epigenetic aging. **Table S7.** Mendelian randomization estimations between epigenetic aging and glaucoma endophenotypes. **Table S8.** Heterogeneity of Mendelian randomization estimations between epigenetic aging and glaucoma endophenotypes. **Table S9.** Pleiotropy of Mendelian randomization estimations between epigenetic aging and glaucoma endophenotypes. **Table S10.** Mendelian randomization estimations between glaucoma endophenotypes and epigenetic aging. **Table S11.** Heterogeneity of Mendelian randomization estimations between glaucoma endophenotypes and epigenetic aging. **Table S12.** Pleiotropy of Mendelian randomization estimations between glaucoma endophenotypes and epigenetic aging.

Acknowledgements
We sincerely appreciate all the participants and investigators of the Edinburgh DataShare, FinnGen, International Glaucoma Genetic Consortium (IGGC), and UK Biobank groups for their valuable contribution to making statistics publicly accessible. The illustrations of diabetic retinopathy, age-related cataract, and glaucoma in Figure 1 were modified from Servier Medical Art (http://smart.servier.com/), licensed under a Creative Common Attribution 3.0 Generic License (https://creativecommons.org/licenses/by/3.0/).

Author contributions
JWC, XLY, and XCD designed the study. JWC and XYL participated in the original draft of the manuscript and literature search. JWC, XY Zhou, and JHX contributed to the formal analysis, investigation, data curation, and visualization. XY Zhou, JHX, XY Zhang, and XCD reviewed and revised the manuscript. XY Zhang and XCD contributed to project administration.

Funding
This work was supported by the Hunan Engineering Research Center for Glaucoma with Artificial Intelligence in the Diagnosis and Application of New Materials, China (Grant No. 2023TP2225 to XD), the Natural Science Foundation of Hunan Province, China (Grant No. 2023JJ70014 to XD), the Changsha Municipal Natural Science Foundation, China (Grant No. kq2208495 to XD), the Science and Technology Foundation of Aier Eye Hospital Group, China (Grant No. AR2206D5 to XD), and the Aier Glaucoma Institute. The funders played no role in the study design, data collection, data analyses, data interpretation, report writing, or decision to publish.

Availability of data and materials
The data for the four epigenetic clocks, DNA methylation proxies for granulocyte proportions, and plasminogen activator inhibitor-1 levels were available from Edinburgh DataShare (https://datashare.is.ed.ac.uk/handle/10283/3645). The summary statistics for AREDs were derived from the FinnGen study, which is available at https://www.finngen.fi/en. The summary data for glaucoma endophenotypes were obtained from the NHGRI-EBI Catalog of human genome-wide association studies (GWAS Catalog, https://www.ebi.ac.uk/gwas/).

Declarations

Conflict of interest
The authors declare no competing interests.

Ethics approval and consent to participate
Ethics approval and consent have been obtained in each original study. Since only publicly available data were used, no additional ethics approval or individual consent was required.

Consent for publication
Not applicable.

Author details
[1]Aier Academy of Ophthalmology, Central South University, Changsha 410015, Hunan Province, People's Republic of China. [2]Changsha Aier Eye Hospital, Changsha 410015, Hunan Province, People's Republic of China. [3]Aier Eye Institute, Changsha 410015, Hunan Province, People's Republic of China. [4]Aier Glaucoma Institute, Hunan Engineering Research Center for Glaucoma With Artificial Intelligence in Diagnosis and Application of New Materials, Changsha Aier Eye Hospital, Changsha, No. 188 South Furong Road, Changsha 410015, Hunan Province, People's Republic of China.

Received: 27 June 2024 Accepted: 7 August 2024
Published online: 14 August 2024

References

1. Voleti VB, Hubschman J-P. Age-related eye disease. Maturitas. 2013;75(1):29–33.
2. Bourne RRA, et al. Magnitude, temporal trends, and projections of the global prevalence of blindness and distance and near vision impairment: a systematic review and meta-analysis. Lancet Glob Health. 2017;5(9):e888–97.
3. Steinmetz JD, et al. Causes of blindness and vision impairment in 2020 and trends over 30 years, and prevalence of avoidable blindness in relation to VISION 2020: the Right to Sight: an analysis for the Global Burden of Disease Study. Lancet Glob Health. 2021;9(2):e144–60.
4. Becker S, et al. Modeling complex age-related eye disease. Prog Retin Eye Res. 2024;100:101247.
5. Jylhävä J, et al. Biological age predictors. EBioMedicine. 2017;21:29–36.
6. Duan R, et al. Epigenetic clock: a promising biomarker and practical tool in aging. Ageing Res Rev. 2022;81:101743.
7. Horvath S. DNA methylation age of human tissues and cell types. Genome Biol. 2013;14(10):R115.
8. Hannum G, et al. Genome-wide methylation profiles reveal quantitative views of human aging rates. Mol Cell. 2013;49(2):359–67.

9. Horvath S, Raj K. DNA methylation-based biomarkers and the epigenetic clock theory of ageing. Nat Rev Genet. 2018;19(6):371–84.
10. Levine ME, et al. An epigenetic biomarker of aging for lifespan and healthspan. Aging (Albany NY). 2018;10(4):573–91.
11. Lu AT, et al. DNA methylation GrimAge strongly predicts lifespan and healthspan. Aging (Albany NY). 2019;11(2):303–27.
12. Gibson J, et al. A meta-analysis of genome-wide association studies of epigenetic age acceleration. PLoS Genet. 2019;15(11):e1008104.
13. Smith GD, Ebrahim S. 'Mendelian randomization': can genetic epidemiology contribute to understanding environmental determinants of disease? Int J Epidemiol. 2003;32(1).
14. Emdin CA, et al. Mendelian randomization. JAMA. 2017;318(19):1925–6.
15. Mccartney DL, et al. Genome-wide association studies identify 137 genetic loci for DNA methylation biomarkers of aging. Genome Biol. 2021;22(1):194.
16. Martínez-Alberquilla I, et al. Neutrophils and neutrophil extracellular trap components: emerging biomarkers and therapeutic targets for age-related eye diseases. Ageing Res Rev. 2022;74:101553.
17. Dan J, et al. Plasminogen activator inhibitor-1 in the aqueous humor of patients with and without glaucoma. Arch Ophthalmol. 2005;123(2):220–4.
18. Lambert V, et al. Influence of plasminogen activator inhibitor type 1 on choroidal neovascularization. FASEB J. 2001;15(6):1021–7.
19. Kurki MI, et al. FinnGen provides genetic insights from a well-phenotyped isolated population. Nature. 2023;613(7944):508–18.
20. Bonnemaijer PWM, et al. Multi-trait genome-wide association study identifies new loci associated with optic disc parameters. Commun Biol. 2019;2:435.
21. Currant H, et al. Genetic variation affects morphological retinal phenotypes extracted from UK Biobank optical coherence tomography images. PLoS Genet. 2021;17(5):e1009497.
22. Pan W, et al. Epigenetic age acceleration and risk of aortic valve stenosis: a bidirectional Mendelian randomization study. Clin Epigenetics. 2024;16(1):41.
23. Wang Z, et al. Effects of iron homeostasis on epigenetic age acceleration: a two-sample Mendelian randomization study. Clin Epigenetics. 2023;15(1):159.
24. Burgess S, Thompson SG. Avoiding bias from weak instruments in Mendelian randomization studies. Int J Epidemiol. 2011;40(3):755–64.
25. Palmer TM, et al. Using multiple genetic variants as instrumental variables for modifiable risk factors. Stat Methods Med Res. 2012;21(3):223–42.
26. Codd V, et al. Identification of seven loci affecting mean telomere length and their association with disease. Nat Genet. 2013;45(4).
27. Hemani G, et al. Orienting the causal relationship between imprecisely measured traits using GWAS summary data. PLoS Genet. 2017;13(11):e1007081.
28. Yoshikawa M, Asaba K. Educational attainment decreases the risk of COVID-19 severity in the european population: a two-sample mendelian randomization study. Front Public Health. 2021;9:673451.
29. Carter AR, et al. Mendelian randomisation for mediation analysis: current methods and challenges for implementation. Eur J Epidemiol. 2021;36(5):465–78.
30. Greco MFD, et al. Detecting pleiotropy in Mendelian randomisation studies with summary data and a continuous outcome. Stat Med. 2015;34(21):2926–40.
31. Burgess S, et al. Guidelines for performing Mendelian randomization investigations: update for summer 2023. Wellcome Open Res. 2019;4:186.
32. Burgess S. Sample size and power calculations in Mendelian randomization with a single instrumental variable and a binary outcome. Int J Epidemiol. 2014;43(3):922–9.
33. Hemani G, et al. The MR-base platform supports systematic causal inference across the human phenome. Elife. 2018;7.
34. Sanderson E, et al. Testing and correcting for weak and pleiotropic instruments in two-sample multivariable Mendelian randomization. Stat Med. 2021;40(25):5434–52.
35. Yavorska OO, Burgess S. MendelianRandomization: an R package for performing Mendelian randomization analyses using summarized data. Int J Epidemiol. 2017;46(6):1734–9.
36. Jayaram H, et al. Glaucoma: now and beyond. Lancet. 2023;402(10414):1788–801.
37. Tham Y-C, et al. Global prevalence of glaucoma and projections of glaucoma burden through 2040: a systematic review and meta-analysis. Ophthalmology. 2014;121(11):2081–90.
38. Chan EWE, et al. Glaucoma in Asia: regional prevalence variations and future projections. Br J Ophthalmol. 2016;100(1):78–85.
39. Zhang Y, et al. Aging, cellular senescence, and glaucoma. Aging Dis. 2024;15(2):546–64.
40. Skowronska-Krawczyk D, et al. P16INK4a upregulation mediated by SIX6 defines retinal ganglion cell pathogenesis in glaucoma. Mol Cell. 2015;59(6):931–40.
41. Chi W, et al. Caspase-8 promotes NLRP1/NLRP3 inflammasome activation and IL-1β production in acute glaucoma. Proc Natl Acad Sci USA. 2014;111(30):11181–6.
42. Xu Q, et al. Stress induced aging in mouse eye. Aging Cell. 2022;21(12):e13737.
43. Liu Y, et al. Senolytic and senomorphic agent procyanidin C1 alleviates structural and functional decline in the aged retina. Proc Natl Acad Sci USA. 2024;121(18):e2311028121.
44. Rocha LR, et al. Early removal of senescent cells protects retinal ganglion cells loss in experimental ocular hypertension. Aging Cell. 2020;19(2):e13089.
45. Mcdonnell FS, et al. Increased global DNA methylation and decreased TGFβ1 promoter methylation in glaucomatous lamina cribrosa cells. J Glaucoma. 2016;25(10):e834–42.
46. Mcdonnell F, et al. Hypoxia-induced changes in DNA methylation alter RASAL1 and TGFβ1 expression in human trabecular meshwork cells. PLoS ONE. 2016;11(4):e0153354.
47. Cai J, et al. Differential DNA methylation patterns in human Schlemm's canal endothelial cells with glaucoma. Mol Vis. 2020;26:483–93.
48. Wan P, et al. TET-dependent GDF7 hypomethylation impairs aqueous humor outflow and serves as a potential therapeutic target in glaucoma. Mol Ther. 2021;29(4):1639–57.
49. Lu Y, et al. Reprogramming to recover youthful epigenetic information and restore vision. Nature. 2020;588(7836):124–9.
50. Chen Q, et al. Associations between the red blood cell distribution width and primary angle-closure glaucoma: a potential for disease prediction. EPMA J. 2019;10(2):185–93.
51. Zeng H-B, et al. The inflammatory cytokine profiles and ocular biometric characteristics of primary angle-closure glaucoma. J Int Med Res. 2023;51(1):3000605221147434.
52. Pan M, et al. Biomechanical correlations between the cornea and the optic nerve head. Invest Ophthalmol Vis Sci. 2024;65(5):34.
53. Chauhan BC, et al. Differential effects of aging in the macular retinal layers, neuroretinal rim, and peripapillary retinal nerve fiber layer. Ophthalmology. 2020;127(2):177–85.
54. Jammal AA, et al. The effect of age on increasing susceptibility to retinal nerve fiber layer loss in glaucoma. Invest Ophthalmol Vis Sci. 2020;61(13):8.
55. Patel NB, et al. Age-associated changes in the retinal nerve fiber layer and optic nerve head. Invest Ophthalmol Vis Sci. 2014;55(8):5134–43.
56. Fleckenstein M, et al. Age-related macular degeneration: a review. JAMA. 2024;331(2):147–57.
57. Strenk SA, et al. The mechanism of presbyopia. Prog Retin Eye Res. 2005;24(3):379–93.
58. Maidana DE, et al. Peripheral monocytes and neutrophils promote photoreceptor cell death in an experimental retinal detachment model. Cell Death Dis. 2023;14(12):834.

Publisher's Note